Exam Challenge : Pressure drop calculation in a heated subchannel

Romain Schmickrath

Nikko Verquin

[Nuclear Thermal Hydraulics]

Prof. Yann Bartosiewicz & Ir. Bert Rossaert

December 6, 2024

I Situation and Objectives

This project aims to develop a 1D model of a BWR (Boiling Water Reactor) subchannel to calculate the pressure drop within it. At the inlet, the fluid is subcooled water with the following conditions: $P_{\text{in}} = 300\,\text{kPa}$ and $T_{\text{in}} = T_{\text{sat}}(P_{\text{in}}) - 40°\text{C}$. A constant heat flux is applied to the pins, and as the fluid flows upward within a prescribed range of mass flow rates ($[0; 2.5]\,\text{kg/s}$), it progressively heats up. This heating process leads to changes in thermodynamic properties and the formation of a vapor phase with a certain fraction (by mass and by volume).

The objective is to determine the thermodynamic properties as a function of the height in the subchannel to compute the pressure drop across the specified range of mass flow rates. To achieve this, several conservation equations and empirical correlations will be employed. The inlet conditions and other parameters of the system are provided in the document *NTH BR 2024 Dec Task Pressure Drop v1.0*.

The heating profile is modeled as a cosine function of the height of the pin, with a maximum value at the center. This is expressed as:

$$\dot{Q}'' = \dot{Q}''_{\text{max}} \times \cos\left(\frac{\pi z}{L}\right) \tag{1}$$

where $\dot{Q}''_{\text{max}} = \dot{Q}_{\text{avg}} \times \frac{\pi}{2}$, and L is the length of the pin.

II Assumptions

In this project, we have made a few assumptions to simplify the calculations.

- The thermodynamic properties of the single-phase fluids, specifically the subcooled liquid and the superheated vapor, are assumed to remain constant. This assumption implies that the saturated vapor and superheated vapor share the same density and viscosity, as do the subcooled liquid and the saturated liquid. The respective values, namely ρ_g and μ_g for vapor and ρ_l and μ_l for the liquid, were determined at saturation conditions and for a pressure equal to the inlet pressure of 300 kPa.
- We assume that the channel operates at a constant pressure, as the pressure drop is negligible in comparison. Specifically, calculations show that the total pressure drop is maximum 1 kPa, while the pressure within the subchannel is 300 kPa.
- We have assumed throughout all the developments made in this project the mechanical equilibrium, which has led to simplifications as $\rho_m = \rho^+$, for which the respective velocities of the two fluids in the two-phase flow is assumed to be equal, $S = 1$.
- We assume thermodynamic equilibrium, so $x_e = x$. We have therefore assumed in our two-phase flow part that flow quality x varies in the same way as equilibrium quality x_e.

- In the case of two-phases flow, we we split the length of the subchannel into 500 intervals of the same length to quantify the evolution of x_e (and therefore x) between Z_B and Z_V. The following formula was used to calculate x_e :

$$x_e = \frac{h - h_L}{h_V - h_L}$$

where h_V and h_L are the enthalpies of the vapor and the liquid at saturation for a pressure of 300 kPa and h varies with height according to the following relationship:

$$h_{\text{out}} = h_{\text{in}} + \frac{Q" P_h z}{\dot{m}}$$

- In order to calculate the density of the mixture (ρ_m) in two-phase flow, we needed the void fraction α which we calculated as follows:

$$\alpha = \frac{\frac{x}{\rho_G}}{\frac{x}{\rho_G} + \frac{1-x}{\rho_L}}$$

this formulation of α therefore assumes that the slip ratio, S, is equal to 1 which is due to our assumption of mechanical equilibrium.

- We assume that liquid phase is incompressible, $\rho_L = const$
- $\mathrm{D}_{\text{hydraulic}} = D_e$

All thermodynamic property values were obtained from the CoolProp database.

III Setting up the Equations and Correlations

In the Figure 1, we can see that the flow of the different phase is a complex behavior. In the aim of this 1D model, simplifications and assumptions are stipulated. In the following part of the report, we will consider three regions of the channel. The first region is the entering section, corresponding to a subcooled liquid. The second region is a subcooled boiling liquid, where the formation of vapor bubbles occurs (below saturation temperature) plus the bulk boiling region, where the fluid is at saturation temperature. Finally, the third region is a vapor region, where the fluid is in a single-phase vapor state.The z-axis of the boiling channel has been discretized into several steps (500) to estimate the fluid properties at each point and calculate the corresponding pressure drop as a function of position.

The equation of the pressure drop is given as a sum of each component inducing a pressure drop in the channel :

$$\Delta p = \Delta p_{\text{acc}} + \Delta p_{\text{gravity}} + \Delta p_{\text{fric}} + \Delta p_{\text{form}} \tag{2}$$

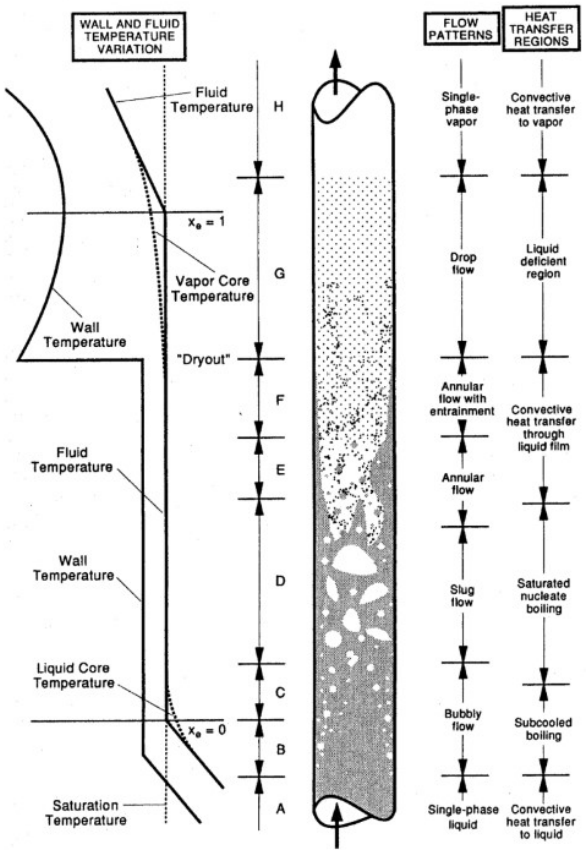

Figure 1: Flow boiling, NTH_{12}

The development of each of these terms gives the total equation :

$$\Delta P = \left(\frac{G_m^2}{\rho_m^+}\right)_{\text{out}} - \left(\frac{G_m^2}{\rho_m^+}\right)_{\text{in}} + \int_{z_{\text{in}}}^{z_B} \rho_L g\, dz + \int_{z_{\text{out}}}^{z_B} \rho_m g\, dz + \frac{\overline{\phi_{Lo}^2} f_{Lo} G_m |G_m| (z_{out} - z_{\text{in}})}{2 D_e \rho_L} (2 \text{ phase})$$

$$+ \frac{f_{Lo} G_m |G_m| (z_B - z_{\text{in}})}{2 D_e \rho_L} (1 \text{ phase}) + \sum_i \left(\frac{G_m |G_m|}{2\rho_L}\right)_i \phi_{Lo}^2 K$$

Where $\overline{\phi_{Lo}^2}(z_{out} - z_D) = \int_{z_{out}}^{z_{in}} \phi_{Lo}^2 dz$ and $\phi_{Lo}^2 = \frac{\rho L}{\rho m} \frac{f_{TP}}{f_{Lo}} \overset{\text{HEM}}{=} \left[1 + x\left(\frac{\rho_{L,sat}}{\rho_{g,sat}} - 1\right)\right]$ (*NTH 10-11, slide 30*)

In the following part, we will neglect the pressure drop due to the drag form, which is usually done in this kind of situation. In order to solve this equation, several correlation must be used and several properties must be known in function of the position, z, in the channel.

Below the height z_B, only the subcooled liquid phase is present, and a transition to subcooled flow boiling is observed in the upper zone. It is important to mention that we do not consider here the onset of nucleated boiling, where bubbles are formed but not detached from the wall, beginning at height z_{NB}. However, this could be calculated using the Rohsenow correlation. The transition at height z_B is given by the Saha-Zuber

correlation (*NTH14, slide 40*) :

$$(\Delta T_{sub})_D = T_{sat} - T_m(z_D) \tag{3}$$

$$\begin{cases} \Delta T_{sub} = 0.0022 \cdot \frac{\dot{Q}'' D_h}{h^h} & \text{if } Pe < 70000 \\ \Delta T_{sub} = 153.8 \cdot \frac{\dot{Q}''}{G m c_p} & \text{if } Pe \geq 70000 \end{cases} \tag{4}$$

Where G_m is the production of the mass flow rate and the cross-section of the channel. From the equation and using the Energy balance, we can obtain z_B :

$$z_B = \frac{G_m De^2 c_p \Delta T_{sub}}{4\dot{Q}" Dh} \tag{5}$$

The friction term for the 2 phase is calculated using the McAdams correlation :

$$f = \begin{cases} 64 & \text{if Re} \leq 2100 \\ 0.184\,\text{Re}^{0.2} & \text{if Re} > 2100 \end{cases} \tag{6}$$

The friction term for the 1 phase is calculated using the Colebrook correlation :

$$\begin{cases} f = 64 & \text{if Re} \leq 2100 \\ \frac{1}{\sqrt{f}} = -2\log_{10}\left(\frac{2.51}{\text{Re}^{0.5}} + 3 \cdot \epsilon^{0.71}\right) & \text{if } 2100 < \text{Re} \leq 1 \times 10^6 \\ \frac{1}{\sqrt{f}} = -2\log_{10}\left(3 \cdot \epsilon^{0.71}\right) & \text{if Re} > 1 \times 10^6 \end{cases} \tag{7}$$

Once each pressure drop terms has been calculated at each discretization step for one flow rate, we sum them over the entire length of the channel to obtain the total pressure drop for the given mass flow rate:

$$\Delta P = \sum_{i=1}^{N} \Delta P_i \tag{8}$$

where ΔP_i represents the sum of each pressure drop term at each discretization step, and $N(= 500)$ is the total number of discretization steps along the length of the channel.

IV Results

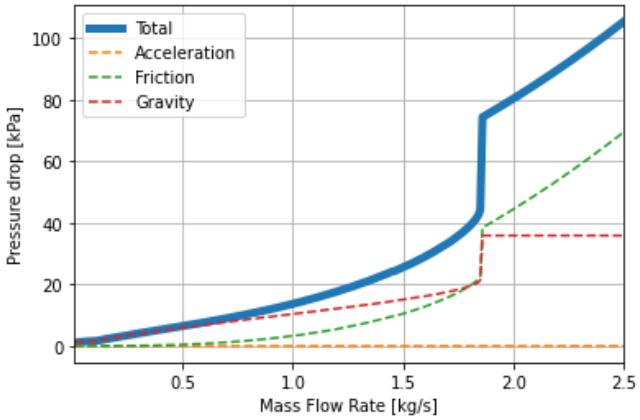

Figure 2: Subcool liquid contribution

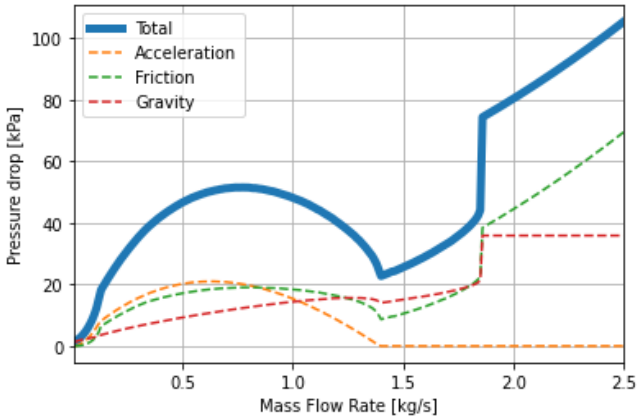

Figure 3: Two phase region contribution

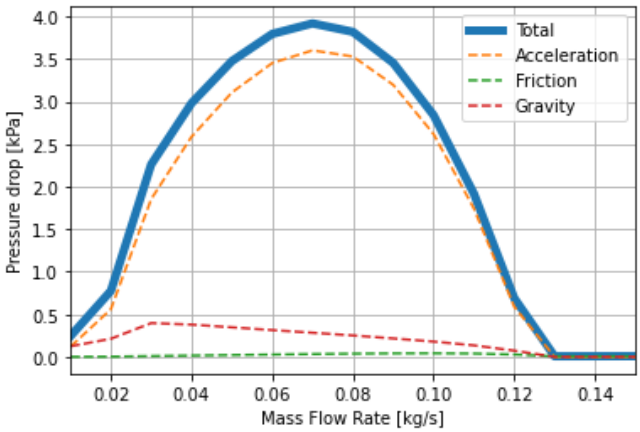

Figure 4: Vapor only contribution

Figure 5: Contribution of each type of flow for the total pressure drop

The three figures above (2, 3, 4) illustrate the combined contributions of the three considered phenomena (gravity, acceleration, and friction) to the total pressure drop across the different regions considered (Liquid only, Two phases, and Vapor only). In general, the liquid phase induces a much higher pressure drop for all components, except for the acceleration term. Indeed, the acceleration term plays a crucial role as long as steam is present in the flow. The temperature gradient leads to significant density variations in the fluid. As the mass flow rate increases and the steam fraction decreases, the contribution of the acceleration term diminishes and nearly vanishes, as the density difference becomes negligible in the liquid phase. This suggests that the subcooled liquid region can be effectively modeled as incompressible. The gravity term is particularly significant for the liquid phase, with its contribution increasing until steam is completely absent from the flow. Beyond this point, it reaches a constant value, as only liquid remains and its density becomes stable. In the vapor-only graph, this curve has a very low absolute value, with a peak at a flow rate of around 0.03 kg/s. Regarding friction, its behavior is influenced by the specific correlations used for modeling, but it generally increases with

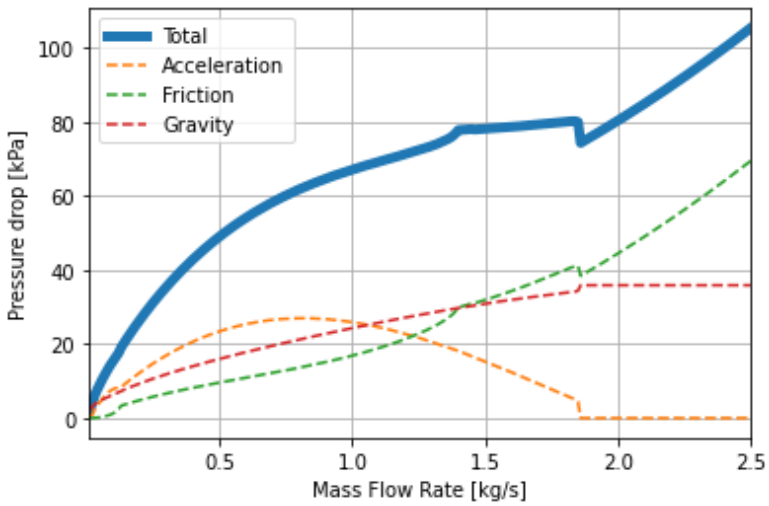

Figure 6: Total pressure drop at different mass flow rate

the fluid mass flow rate, as expected. A decrease in friction with an increasing steam fraction is also observed, though it is important to note the scale of each graph. The discontinuities observed in the friction term are due to changes in the applied correlations, which may not always ensure a smooth transition. Additionally, the friction pressure drop in the vapor phase is almost zero for any flow rate. In the vapor-only graph, the pressure drop becomes zero after a flow rate of approximately 0.13 kg/s. This observation aligns logically with Figure 7b. Indeed, in this figure, we see that beyond a flow rate of approximately 0.12 kg/s, the superheated height exceeds the total height of the channel. At such high flow rates, the fluid does not have enough time to completely form vapor, whether saturated or superheated, depending on the situation.

The figure 6 represents the total pressure drop compared to the mass flow rate. At lower mass flow rates, acceleration is a significant contributor to the total pressure. As the mass flow rate increases, friction becomes the dominant factor driving the pressure drop. Gravity remains constant and contributes a fixed amount throughout the range of flow rates. Those can be explained by the same ways as we did previously explained the three different pressure losses. We can conclude that

V Extra Results

V.1 Boiling Height and Superheated Height in function of mass flow rate

In this section, we plotted the heights of z_B and z_V as functions of the mass flow rate. It can be observed that for the superheated region, once the flow rate exceeds 0.12 kg/s, the value of z_V no longer exists within the height range of the channel. This is entirely logical, as an increase in the mass flow rate reduces the time available for the fluid to heat up and undergo evaporation. Moreover, we observe that for the boiling height, this mass flow rate limit is higher, which is also logical.

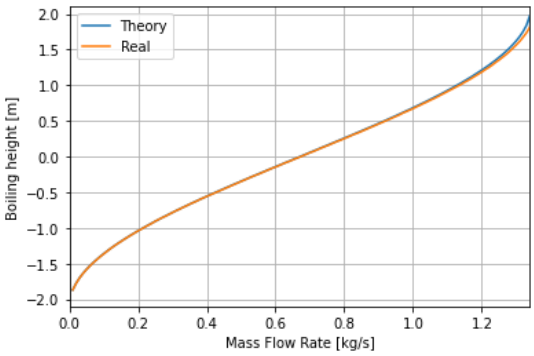

(a) Boiling Height vs mass flow rate

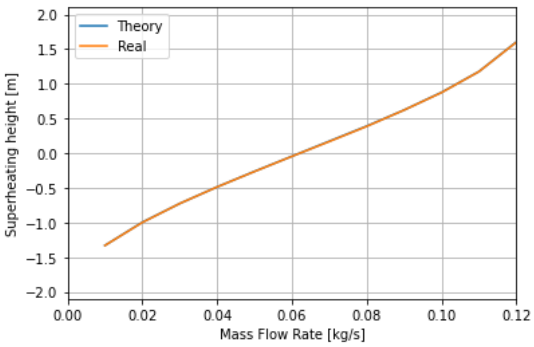

(b) Superheated Height vs mass flow rate

V.2 Equilibrium and flow quality in terms of height for a mass flow of 0,1 kg/s

The graph illustrates the variation of equilibrium quality (x_e) and flow quality (x) as a function of channel height for a mass flow rate of 0.1 kg/s.

The graph illustrates the variation of equilibrium quality (x_e) and flow quality (x) as a function of channel height for a mass flow rate of 0.1 kg/s. At low channel heights, the flow quality is slightly higher than the equilibrium quality, indicating a lag in thermal equilibrium or faster vapor formation than equilibrium predictions. As the height increases, both x and x_e converge, suggesting that the system approaches equilibrium. This behavior reflects the gradual vaporization of the liquid phase as heat is transferred along the channel height.

Additionally, it is observed that x_e can take on negative values when the temperature (average) is below the saturation temperature at the inlet pressure. This indicates the subcooled liquid region, where no vapor is present, and the equilibrium quality reflects the deviation from saturation conditions. On the other hand, x cannot be negative and is limited to zero, as flow quality represents the physical ratio of vapor to total mass, which cannot be less than zero. Furthermore, both x_e and x can exceed one under certain conditions, particularly in the superheated region where all the liquid has vaporized, and additional heating increases the vapor temperature. However, in reality, once x reaches a

value of 1, the channel contains only vapor, and the notion of quality beyond this point is not really useful anymore.

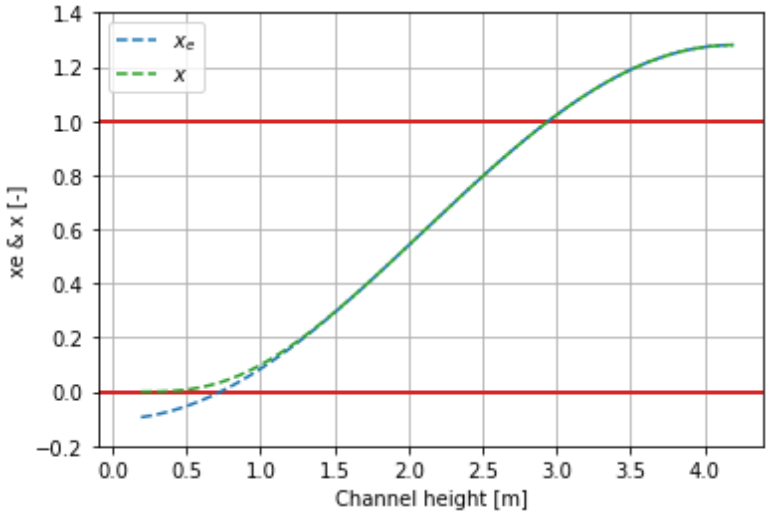

Figure 8: Equilibrium and flow quality in terms of height for a mass flow of 0,1 kg/s

In order to reduce the 'S-shape' of our curves, we must play on the pressure. Indeed, it is the phase transition that induce this kind of shape. By increasing the pressure, the boiling point is raised, which changes the phase transition curve. At higher pressures, the curve becomes less pronounced because the system operates in a more superheated or subcooled region, thus eliminating the 'S- shape'.

V.3 Jones' correlation alternative for the two phase friction pressure drop

The Jones' correlation for calculating the two-phase friction multiplier is given by:

$$G_m = \frac{\dot{m}}{A_{\text{flow}}} \quad [\text{kg/m}^2\text{s}]$$
$$p_{\text{int}} = p \cdot 0.000145038 \quad [\text{psi}]$$

The factor Ω is defined as:

$$\Omega = \begin{cases} 1.36 + 0.0005\, p_{\text{int}} + G_m \cdot 10^{-6} \cdot (0.1 - 0.000714\, p_{\text{int}}), & \text{if } G_m \leq 0.7 \cdot 10^6 \\ 1.26 - 0.0004\, p_{\text{int}} + \frac{1}{G_m \cdot 10^{-6}} \cdot (0.119 + 0.00028\, p_{\text{int}}), & \text{if } G_m > 0.7 \cdot 10^6 \end{cases}$$

The two-phase friction multiplier is then calculated as:

$$\phi_{lo}^2 = \Omega \cdot \left[1.2 \cdot \left(\frac{\rho_l}{\rho_g} - 1 \right) \cdot x^{0.824} \right] + 1$$

In this section, we plot the pressure drop in the same manner as done in the "Results"

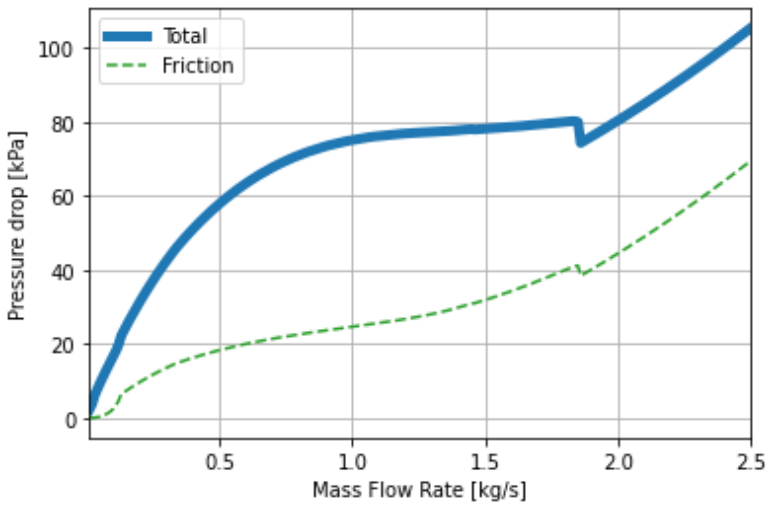

Figure 9: Total pressure drop calculated with Jones' correlation

section. However, this time, the two-phase multiplier is calculated using Jones' correlation, as presented above. The resulting Figure is shown below (see Figure 9 and can be compared to the results from the previous graph 6. At first, the two graphs appear similar, displaying the same overall shape. However, upon closer inspection, we can observe that the friction term differs in the two-phase zone. This is the region where the pressure drop due to friction is affected. The impact is particularly noticeable at lower mass flow rates, typically below 1.5 kg/s, where the Jones correlation predicts a higher frictional pressure drop, approximately 20-40% greater, depending on the flow rate (with the effect being more significant at lower flow rates). For flow rates above 1.8 kg/s, however, the friction curves in both cases converge, showing the same trend.